Available online at www.sciencedirect.com

ScienceDirect

Scripta Materialia 106 (2015) 17–20

Scripta MATERIALIA

www.elsevier.com/locate/scriptamat

Latent hardening effect under self- and coplanar dislocation interactions in Mg single crystals

F. Hiura and M. Niewczas*

Materials Science and Engineering, McMaster University, Hamilton, Canada

Received 4 March 2015; revised 9 April 2015; accepted 12 April 2015
Available online 30 April 2015

Latent hardening experiments were carried out on Mg single crystals under basal self- and coplanar dislocation interactions. For self-interactions the latent hardening ratio (*LHR*) is independent on the amount of primary deformation in the basal slip system. For coplanar interactions *LHR* increases linearly with primary strain and quadratically with primary stress, suggesting that during the stage A in Mg the coplanar slip systems harden proportionally to the dislocation density accumulated in the other coplanar slip system.

Keywords: Magnesium single crystals; Easy glide; Basal slip; Latent hardening; Coplanar interactions

During plastic flow of crystalline materials, an active slip system exerts the strength on inactive slip systems; this process is known as latent hardening and it plays an important role in crystal plasticity [1]. The latent hardening effect has been studied extensively in FCC single crystals of pure metals and alloys under uniaxial tension and compression [2–10], pure shear [11–14] and cyclic fatigue [15,16]. In the experiments on Cu single crystals, Jackson and Basinski [4,17,18] observed strong hardening effect due to forest interactions between non-coplanar slip systems, but no hardening during interactions between coplanar systems. Pure shear experiments on Cu show that during the early stages of plastic flow the strengthening of coplanar slip systems increases with increasing deformation in the primary system [13]. Subsequent studies of latent hardening in Al and Cu single crystals [9] revealed that the coplanar interactions exhibit features similar to those observed during hardening under non-coplanar interactions namely, initial increase of the strength in the coplanar systems during early stage I of work-hardening, followed by its decrease to some constant value later in stage II.

HCP materials display different plastic flow attributes than FCC materials, determined by strong flow anisotropy of available deformation modes and polarized nature of twinning. In Mg single crystals, basal slip is dominant deformation mechanism in a wide range of orientations and over a broad range of temperatures [19–24]. The interactions of basal slip with other slip and twinning systems occur frequently during plastic flow and control the work-hardening of Mg. This makes it difficult to determine the latent hardening effects under non-basal slip or twin interactions. Pure shear experiments carried out on Zn [25,26], Cd [25] and Mg [27] single crystals are consistent with results obtained on FCC materials [13] and suggest that for small deformations, the hardening of coplanar slip systems increases approximately linearly with the primary shear strain. In the present work we study latent hardening effect in Mg single crystals under conditions of self- and coplanar basal dislocation interactions and extend these studies to the limit of easy glide in tension at room temperature. The scaling relationship governing the strength of the interactions is analyzed.

High purity Mg single crystals of dimension $\sim 3 \times 26 \times 120\ mm^3$ were grown in spectroscopically pure graphite mold by a modified Bridgman method, under argon atmosphere. The crystals were deformed in tension at room temperature to some predetermined levels of strain with the constant strain rate of $1 \times 10^{-4}\ s^{-1}$. After unloading, secondary samples were spark-cut from the pre-strained parent crystals to promote a single coplanar slip system during secondary tensile deformation. The cross-section of the secondary samples was kept $\sim 3 \times 3\ mm^2$, with the gauge length dependent on the sample orientation and deformation mode, typically not less than 15 mm. To remove spark damage, spark-cut faces of the secondary samples were chemically polished, followed by electro-chemical polishing of the specimens in the same solutions as the parent crystals. The secondary samples were deformed in tension at room temperature with the strain rate of $1 \times 10^{-4}\ s^{-1}$. The slip marking patterns formed on the lateral surfaces of parent and secondary samples were studied under optical microscope with Nomarski contrast.

* Corresponding author. e-mail: niewczas@mcmaster.ca

http://dx.doi.org/10.1016/j.scriptamat.2015.04.008
1359-6462/

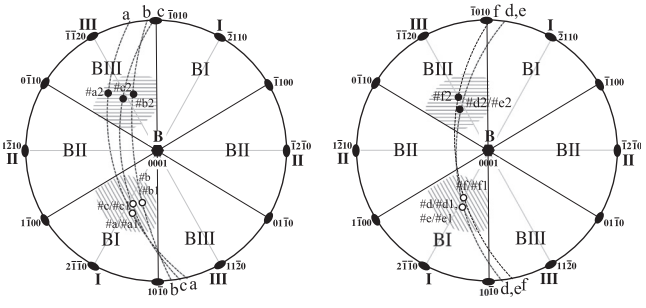

Figure 1. (0001) standard stereographic projection depicting the orientation of the tensile axis of parent single crystals #a–#f and secondary samples #a1–#f1, #a2–#f2 and the trace of the wide face of the parent crystals ((a–a)–(e–e)). The Miller–Bravais indices of crystallographic plans and directions in hexagonal system are related as: $[uvtw] = [hki(l/\lambda^2)]$ and $(hkil) = (uvt(\lambda^2 w))$, where $\lambda^2 = 2/3(c/a)^2 = 1.757$ for Mg. The corresponding crystallographic directions of the tensile axis for all samples are given in Tables 1 and 2.

Figure 1 shows (0001) standard stereographic projection depicting the orientation of the tensile axis of parent crystals and secondary samples, given in terms of the crystallographic plane normal to the tensile axis. BI, BII and BIII denote three basal slip systems, $(0001)[2\bar{1}\bar{1}0]$, $(0001)[\bar{1}2\bar{1}0]$ and $(0001)[\bar{1}\bar{1}20]$ respectively. The range of crystallographic orientations where these systems are expected to be active during plastic flow are depicted by the stereographic triangles labeled BI, BII and BIII in Figure 1. The homogeneous deformation of Mg single crystals under a single basal slip is limited to the specific areas in the orientation space for which the angle between the slip direction and the tensile axis of the crystals is within 40°–60° [19]. If this angle is too large or too small, inhomogeneous deformation associated with kink bands formation and deformation twinning occurs in addition to the basal slip [19–21]. The dashed areas on the stereographic projection in Figure 1 represent "safe" regions for the homogeneous deformation of crystals under the basal slip. The open circles in Figure 1 depict the crystallographic orientations of the tensile axis of as-grown parent single crystals #a–#f and the secondary samples #a1–#f1 cut form the parent crystals, with the same orientation of the tensile axis. For all these orientations, the Schmid factor for basal slip is in the range 0.47–0.50, high enough to promote a homogeneous deformation of crystals in a single basal slip system; this has been verified by microscopy observations of slip marking patterns formed on the lateral surfaces, not shown here. The orientation of the secondary samples can be selected by suitable rotation around normal to the wide face of the parent crystals along the great circles labeled as "a–a"–"f–f" in Figure 1, representing the trace of the crystals' wide faces. The samples #a1–#f1 cut parallel to the tensile axis of the pre-deformed parent crystals were used to investigate interactions between the same type of dislocations activated in the secondary tensile test, as those stored in the sample after primary deformation plus the effect of stress relaxation due to sample unload on the flow stress. The secondary samples #a2–#f2 were oriented approximately at 90° with respect to the axis of the parent crystals #a–#f to promote the coplanar basal slip system BIII (Fig. 1) during secondary tensile test, with the Burgers vector at 120° to the Burgers vector of BI dislocations.

Figure 2 shows the variations of the Schmid factor for the basal slip systems BI, BII and BIII against the rotation angle around the normal to the wide face in crystal #c. The tensile axis of the parent sample #c, corresponding to 0° rotation angle in Figure 2, is used as the reference direction, with the clockwise rotation defined as $+\theta$ and the anti-clockwise rotation, as $-\theta$. The Schmid factor for basal BI slip system assumes the value −0.48 at 0° rotation angle, which produces the highest resolved shear stress on BI slip system. As the θ increases in the clockwise direction, the absolute value of m for BI slip system decreases and for BIII slip system increases. At rotation angle $\theta = 90°$, the Schmid factor for BIII slip system $m = -0.49$, producing highest resolved shear stress acting on it. Following this procedure, the orientation of all secondary samples was chosen to be within a dashed zone of high Schmid factor for homogeneous deformation in a single basal BIII slip system, as shown in Figure 1.

Figure 3 shows $\tau - \gamma$ (Fig. 3(a)) and $\theta - \gamma$ characteristics (Fig. 3(b)) for parent crystals deformed within stage A of easy glide and secondary samples #c1 and #c2 cut from the parent crystals for latent hardening experiments. The flow stress and the work-hardening rate of the parent samples during stage A is strongly dependent on crystal orientation and the contribution of non-basal slip systems to the plastic flow (Table 1). For the parent crystal #c, the work-hardening decreases monotonically during the onset of easy glide from $1.5 \times 10^{-4}\mu$ to $5 \times 10^{-5}\mu$ at the end of stage A. The secondary samples #c1 and #c2, cut from the pre-deformed parent crystals, exhibit qualitatively similar flow stress characteristics. Their work-hardening rate decreases somewhat faster than that observed in parent samples, also from $\sim 1.5 \times 10^{-4}\mu$ down to $\sim 5 \times 10^{-5}\mu$, at a later stage of plastic flow (Fig. 3(b)). The results suggest that the same kinds of interactions control the work-hardening in parent and secondary samples. The strength of the interactions between different slip systems is usually characterized by the latent hardening ratio $LHR = \tau_0^j/\tau_{max}^i$, defined as the ratio of the initial resolved shear stress of secondary sample τ_0^j, over the final resolved shear stress of the parent crystal τ_{max}^i [4]. Figure 4 shows *LHRs* as a function of the primary strain and as a function of the effective stress in the primary basal BI slip system, under conditions of self-interactions between systems BI/BI and during coplanar interactions between systems BI/BIII. Each point is plotted as the mean value of several measurements with the error indicated by the standard deviation. It is seen that *LHR* during BI/BI self-interactions is independent on the applied strain and/or stress in the primary deformation and $LHR \approx 1$. The *LHRs* for coplanar BI/BIII interactions shows linear increase with

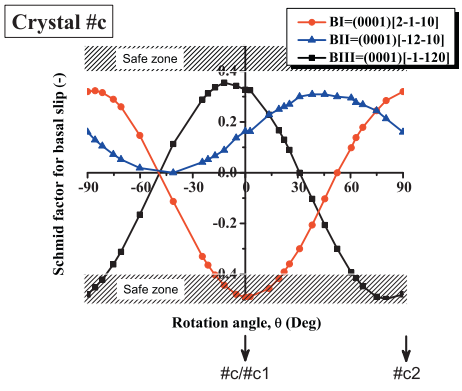

Figure 2. Variations of the Schmid factor for the basal slip systems BI, BII and BIII as a function of rotation angle around the normal to the wide face in crystal #c. The reference direction, 0° rotation angle, is the direction of the tensile axis of crystal #c.